Molecular Biology of the Cell
Vol. 20, 296–305, January 1, 2009

Disruption of the Interaction between Transcriptional Intermediary Factor 1β and Heterochromatin Protein 1 Leads to a Switch from DNA Hyper- to Hypomethylation and H3K9 to H3K27 Trimethylation on the *MEST* Promoter Correlating with Gene Reactivation

Raphaël Riclet,* Mariam Chendeb,* Jean-Luc Vonesch,* Dirk Koczan,† Hans-Juergen Thiesen,† Régine Losson,* and Florence Cammas*

*Institut de Génétique et de Biologie Moléculaire et Cellulaire, Centre National de la Recherche Scientifique/Institut National de la Santé et de la Recherche Médicale/Université Louis Pasteur/Collège de France, 67404 Illkirch-Cedex, France; and †Institute for Immunology, Medical Faculty, 18057 Rostock, Germany

Submitted May 22, 2008; Revised September 26, 2008; Accepted October 3, 2008
Monitoring Editor: Wendy Bickmore

Here, we identified the imprinted mesoderm-specific transcript (*MEST*) gene as an endogenous TIF1β primary target gene and demonstrated that transcriptional intermediary factor (TIF) 1β, through its interaction with heterochromatin protein (HP) 1, is essential in establishing and maintaining a local heterochromatin-like structure on *MEST* promoter region characterized by H3K9 trimethylation and hypoacetylation, H4K20 trimethylation, DNA hypermethylation, and enrichment in HP1 that correlates with preferential association to foci of pericentromeric heterochromatin and transcriptional repression. On disruption of the interaction between TIF1β and HP1, TIF1β is released from the promoter region, and there is a switch from DNA hypermethylation and histone H3K9 trimethylation to DNA hypomethylation and histone H3K27 trimethylation correlating with rapid reactivation of *MEST* expression. Interestingly, we provide evidence that the imprinted *MEST* allele DNA methylation is insensitive to TIF1β loss of function, whereas the nonimprinted allele is regulated through a distinct TIF1β–DNA methylation mechanism.

INTRODUCTION

Cell functions result from the interpretation of genetic and epigenetic information established by a large cohort of complexes acting at the chromatin level (reviewed in Mellor, 2006). Gene silencing, in particular, plays essential roles during development and cell differentiation that require progressive extinction of pluripotent genes and specific cell lineage genes (reviewed in Rajasekhar and Begemann, 2007). Several histone modifications, believed to establish a "histone code," are thought to be essential in this silencing program; these modifications include H3K9 trimethylation (3meH3K9) and H4K20 trimethylation (3meH4K20), two modifications well known to be associated with heterochromatin structures (Schotta *et al*., 2004; Grewal and Jia, 2007); H3K27 trimethylation (3meH3K27), a mark assumed to be associated with facultative heterochromatin and to be particularly enriched in polycomb response elements (Bracken *et al*., 2006). Moreover, recent studies indicate that different combinations of these and other histone marks can lead to different outputs that are difficult to anticipate considering the complexity of this combinatorial code (reviewed in Hirose, 2007; Reik, 2007). Another key epigenetic modification is DNA methylation that has well-characterized functions in genomic imprinting, X chromosome inactivation, silencing of tumor suppressor genes, and repression of viral elements (reviewed in Latham *et al*., 2008). It has been predicted that ~6% of CpG islands display tissue- and or developmental stage-specific DNA methylation pattern (Song *et al*., 2005; Weber *et al*., 2007). Although DNA methylation correlates with gene repression, the functional relevance of this level of regulation remains largely to be established in vivo.

Among complexes known to be involved in establishing gene silencing are those containing the transcriptional corepressor, TIF1β (Transcriptional Intermediary factor 1β), that plays essential roles during early embryonic development and terminal cell differentiation (Cammas *et al*., 2000; 2004). TIF1β (Le Douarin *et al*., 1996) (also known as KAP-1, Friedman *et al*., 1996; or TRIM28) is the universal corepressor for the Krüppel-associated box domain containing zinc-finger proteins (KRAB-ZFP) family of transcription factors that constitutes the largest family of repressors in mammals (Friedman *et al*., 1996; Kim *et al*., 1996; Moosmann *et al*., 1996; Abrink *et al*., 2001). TIF1β is an intrinsic component of two chromatin remodeling and histone deacetylase complexes, N-CoR1 and NuRD (Underhill *et al*., 2000; Schultz *et al*., 2001) and directly interacts with the histone methyltransferase SETDB1, which specifically methylates H3K9 preferentially within euchromatin (Schultz *et al*., 2002). TIF1β also interacts with members of the heterochromatin protein (HP) 1 family through a specific pentapeptide

This article was published online ahead of print in *MBC in Press* (http://www.molbiolcell.org/cgi/doi/10.1091/mbc.E08–05–0510) on October 15, 2008.

Address correspondence to: Régine Losson (losson@igbmc.u-strasbg.fr).

PxVxL called HP1box (Le Douarin *et al*., 1996; Nielsen *et al*., 1999; Ryan *et al*., 1999; Thiru *et al*., 2004; Cammas *et al*., 2007). HP1 is a structurally and functionally highly conserved protein with family members found in eukaryotic organisms ranging from *Schizosaccharomyces pombe* to humans (Eissenberg *et al*., 1990; Wang *et al*., 2000). These proteins participate in chromatin packaging and have a well-established function in heterochromatin-mediated silencing (reviewed in Grewal and Jia, 2007). More recent data suggest that HP1 functions are much more diversified than initially assumed. These functions include gene specific silencing (Cryderman *et al*., 2005; Smallwood *et al*., 2007), gene activation (Cryderman *et al*., 2005), and transcriptional elongation (Vakoc *et al*., 2005). Mice and humans have three different HP1 proteins (HP1α, β, and γ) that are associated, although not exclusively, with pericentromeric heterochromatin (Nielsen *et al*., 1999). It is currently speculated that HP1 serves as a bridging protein, connecting histones to nonhistone chromosomal proteins through specific recognition of di- and trimethylated H3K9 by the HP1 chromodomain and association with diverse proteins through their HP1box and HP1 chromoshadow domain (Lomberk *et al*., 2006). We and others have demonstrated previously that the interaction between TIF1β and HP1 is required for 1) TIF1β transcriptional repression activity, which also requires histone deacetylase activity (Nielsen *et al*., 1999; Ryan *et al*., 1999); 2) relocation of TIF1β from euchromatin to heterochromatin that accompanies the retinoic acid (RA)-induced primitive endodermal (PrE) differentiation of mouse embryonal carcinoma F9 cells (Cammas *et al*., 2002) and for 3) progression through F9 cell differentiation into RA plus cAMP-induced parietal endodermal differentiation (Cammas *et al*., 2004). Up to now, the molecular mechanisms underlying TIF1β functions as a corepressor of the KRAB-ZFP have been assessed in reporter systems (Ayyanathan *et al*., 2003; Sripathy *et al*., 2006). In these studies, the authors demonstrated that the artificial recruitment of TIF1β to the promoter region of a reporter gene induces stable silencing through the establishment of a heterochromatin-like structure characterized by trimethylation of the H3K9, DNA methylation, and HP1 recruitment that is maintained for several generations.

In the present study, we identified mesoderm-specific transcript (*MEST*) as an endogenous TIF1β primary target gene and characterized the influence of the interaction between TIF1β and HP1 on its expression, its chromatin structure, and its nuclear positioning.

MATERIALS AND METHODS

Details on individual plasmid constructs, which were all verified by sequencing, are available upon request.

Antibodies

Antibodies used in this study were as follows: mouse anti-TIF1β monoclonal antibody (mAb), 1Tb3, raised against recombinant *Escherichia coli* expressed mouse TIF1β (123-834) (Nielsen *et al*., 1999); rabbit anti-TIF1β polyclonal antibody (pAb), PF64, raised against TIF1β (amino acids 141–155; Cammas *et al*., 2002); mouse anti-FLAG mAb 2FLB11; anti-HP1α mAb 2HP-2G9; and anti-HP1β mAb 1MOD-1A9; anti-HP1γ mAb, 2 Mod-1G6 (Nielsen *et al*., 1999). The antibodies specific for the different histone modifications were purchased from Millipore (Billerica, MA).

Cell Culture

Wild-type (WT) and mutant F9 cells were grown as monolayers in DMEM (Invitrogen, France) supplemented with 10% fetal calf serum as previously described (Boylan and Gudas, 1991). Cells were counted with a particle counter (Coulter Z2).

Immunoprecipitation and Western Blot Analysis

Isolation of whole cell extracts from F9 cells and Western blot detection were performed as described previously (Chiba *et al*., 1997; Nielsen *et al*., 1999).

Reverse Transcription-Polymerase Chain Reaction (RT-PCR)

RNA extraction was performed with TRIzol reagent (Invitrogen). *MEST* cDNA was amplified with AHY249 (5′-GAAATTCAGAAGACGCTGGG-3′) and AHN102 (5′-CTCCAAAAACTCTGGATACG-3′); *PEG3* cDNA with BBJ400 (5′-CCTGATCAATGGGTTCCTTG-3′) and BBJ401 (5′-CTTCTGGAAGCCGACATTATG-3); *PEG10* cDNA with BBJ402 (5′-CGAGTGTACTTATTGGTCCC-3′) and BBJ403 (5′-TGACTGTCATCTGGCATTCC-3′); *COPG2* cDNA with BBH298 (5′-CTTGCTGTCTCCAACATG-3′) and BBH299 (5′-ATTTCGCAAGCAGCTCTC-3′); *MEG3* cDNA with BBZ369 (5′-GACTTCACGCACAACACG-3′) and BBZ370 (5′-ACAAGGGCGCTTCCAATC-3′); *IGF2R* cDNA with BAM406 (5′-CAAAGGGAAGAGCTATGATG-3′) and BAM407 (5′-ATCTTCACTTTCATCACACG-3′); and *HPRT* cDNA with QG197 (5′-GTAATGATCAGTCAACGGGGGAC-3′) and QG198 (5′-CCAGCAAGCTTGCAACCTTAACCA-3′).

Chromatin Immunoprecipitation (ChIP) Assay

ChIP assays were performed according to the Millipore protocol with some minor modifications. Cells were cross-linked with 1% formaldehyde for 10 min at 37°C resuspended in lysis buffer (0.1% SDS, 50 mM HEPES, pH 7.9, 140 mM NaCl, 1 mM EDTA, 1% Triton X-100, and 0.1% Na-deoxycholate) at a final concentration of 12.5×10^6 cells/500 μl, incubated on ice for 10 min, and sonicated to average fragment size of 200–500 base pairs. The clarified solubilized chromatin was diluted fivefold in ChIP dilution buffer (16.7 mM Tris-HCl, pH 8.1, 1.2 mM EDTA, 167 mM NaCl, 0.01% SDS, and 1.1% Triton X-100). Immunoprecipitation was performed with 8 μl of mAb (TIF1β and HP1), 10 μl of pAb (TIF1β), or 3 μl of pAb (histone modifications). The beads were washed sequentially once with low salt buffer (20 mM Tris-HCl, pH 8.1, 2 mM EDTA, 150 mM NaCl, 0.1% SDS, and 1% Triton X-100), high salt buffer (20 mM Tris-HCl, pH 8.1, 2 mM EDTA, 500 mM NaCl, 0.1% SDS, and 1% Triton X-100), LiCl buffer (10 mM Tris-HCl, pH 8.1, 1 mM EDTA, 0.25 M LiCl, 1% NP40, and 1% deoxycholate) and twice with TE buffer (10 mM Tris-HCl, pH 8.0, and 1 mM EDTA). Immunocomplexes were eluted twice with 250 μl of elution buffer (1% SDS and 0.1 M $NaHCO_3$) for 15 min at RT. Eluates and input chromatin were heated at 65°C overnight in the presence of 0.2 M NaCl. ChIP DNA were quantified by real-time PCR using the QuantiTect SYBR Green Kit (QIAGEN, Hilden, Germany), and the final results for each sample were normalized to the inputs. PCR reactions were performed in triplicate in a LightCycler (Roche Diagnostics, Mannheim, Germany) with 3 μl of ChIP DNA. Primer sequences for the *MEST* promoter were as follows: forward, 5′-CAGCAGCTTCTGGCATGTGG-3′ and reverse, 5′-AACCCCAGATTCTAGTGAAG-3′; for the region 5′ 10 kb upstream of the *MEST* promoter: forward, 5′-TGGTGGCAGATGACTGTTAG-3′ and reverse, 5′-GAAGAATAGGCAATGCAGTG-3′; for the region 5′ 4 kb upstream of the *MEST* promoter: forward, 5′-ATCTGCAGTTTTGCCTCAGG-3′ and reverse, 5′-ATGAAGGCACACAGAGATGC-3′; for the region 3′ 5 kb downstream of the *MEST* promoter: forward, 5′-TTTCCTGAGACGCATCGTCC-3′ and reverse, 5′-ATAGACTGGCTCATCACCAC-3′; for the *HPRT* promoter: forward, 5′-TTATCTGGGAATCCTCTGGG-3′ and reverse, 5′-AAAGGCAGTTCCGGAACTCT-3′; and for the major satellites: forward, 5′-GACGACTTGAAAAATGACGAAATC-3′ and reverse, 5′-CATATTCCAGGTCCTCAGTGTGC-3′.

DNA Fluorescence in Situ Hybridization (FISH)

Wild-type and mutant F9 cells were grown on gelatin-coated coverslips for 72h washed for 5 min in 1× PBS, fixed in 2% paraformaldehyde 10 min at room temperature (RT). Coverslips were treated with 0.1 M Tris-Cl, pH 7.2, for 10 min at RT and washed in 1× phosphate-buffered saline (PBS) for 5 min. Cells were permeabilized for 10 min at RT with 1× PBS, 0.1% Triton X-100, and 0.1% saponin, and then they were incubated in 20% glycerol, 1× PBS solution for 20 min. Coverslips were immersed three times in liquid nitrogen and allowed to thaw at RT, washed 5 min in 1× PBS, and treated with 100 μg/ml DNase-free RNase A in 1× PBS for 1 h at 37°C. Coverslips were washed in 1× PBS for 5 min and then in 1× PBS, 0.1% Triton X-100, and 0.1% saponin for 30 min at RT. Coverslips were then washed in 1× PBS, dehydrated by an ethanol series (80, 90, and 100%) for 3 min each, and air-dried. Seven microliters of hybridization cocktail containing 100 ng of dCTP-Cy3 (GE Healthcare, Little Chalfont, Buckinghamshire, United Kingdom)-labeled probe, 4 μg of mouse Cot-1 DNA, 1 μg of sheared salmon-sperm DNA in 50% formamide, 2× SSC, and 10% dextran sulfate was heated at 76°C for 10 min and added to each coverslip. Coverslips were mounted on slides, and DNA-probe and cellular DNA were denatured simultaneously on a hot block at 75°C for 3 min and hybridized in a humid atmosphere at 37°C for 24 h. On the following day, coverslips were washed once in 50% formamide, 2× SSC, pH 7.5, for 20 min, three times in 0.1× SSC 5 min each at 37°C, once in 0.1% Tween 20, 4× SSC for 5 min at 45°C, and finally in 1× PBS for 5 min at RT, stained for DNA with Hoechst 33258 at 5 μg/ml and mounted in PBS 5% propyl gallate, 80% glycerol. Images acquisition was performed using a Leica

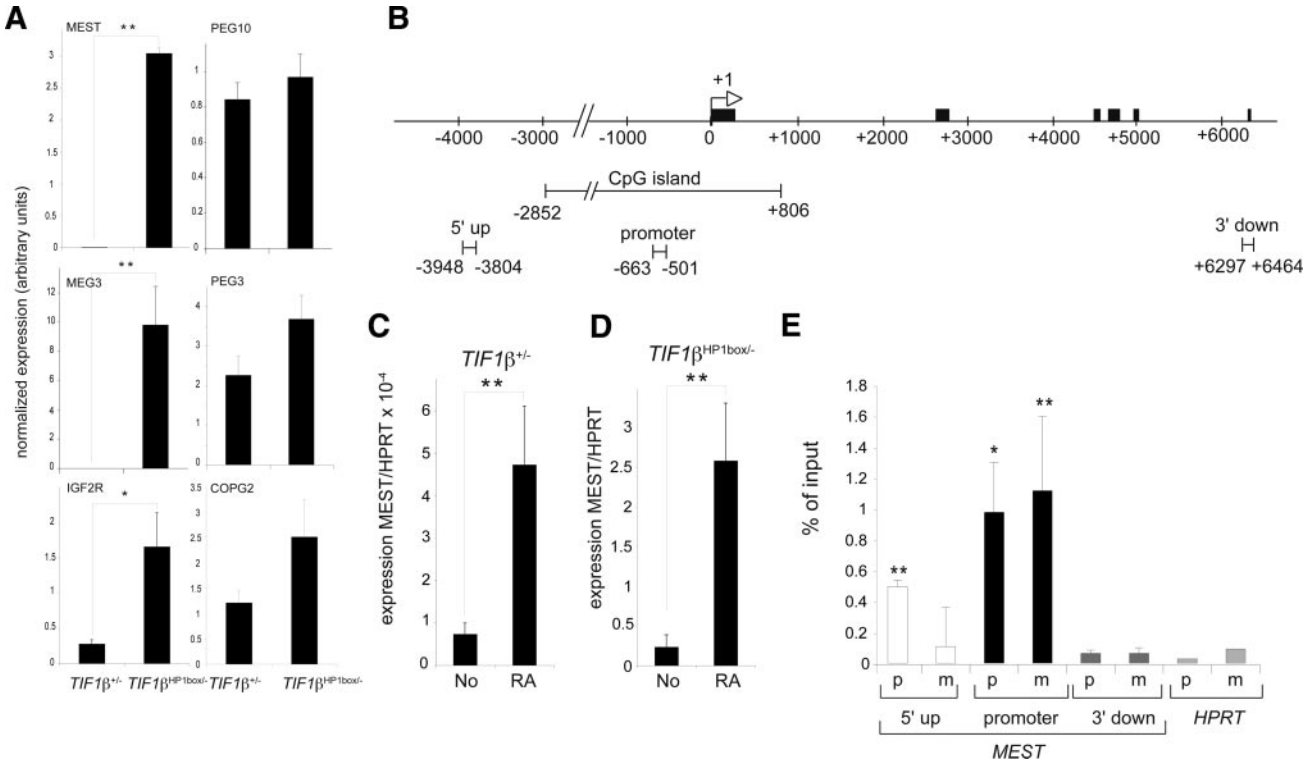

Figure 1. MEST is a TIF1β primary target gene. (A) Expression of *MEST* (*PEG1*), *PEG3*, *PEG10*, *MEG3*, *IGF2R*, and *COPG2* was assessed in *TIF1*$\beta^{+/-}$ and *TIF1*$\beta^{HP1box/-}$ F9 cells by RT-PCR analysis. *HPRT* was used as a control house-keeping gene. (B) Schematic representation of the *MEST* gene with the black boxes representing the exons. The arrow labeled + 1 represents the transcription start site described in Lefebvre *et al*. (1997). The different regions amplified for the ChIP analysis are shown. (C and D) RA-inducible expression of *MEST* is independent of TIF1β–HP1 interaction. *TIF1*$\beta^{+/-}$ (C) and *TIF1*$\beta^{HP1box/-}$ (D) cells were treated for 96 h with either ethanol (no) or 1 μM all-*trans* RA (RA). *MEST* expression was measured by qRT-PCR and normalized with *HPRT* expression. (E) ChIP assay with two anti-TIF1β antibodies (p, PF64 pAb; m, 1TB3 mAb) was performed in WT EC F9 cells. The three positions analyzed on the *MEST* gene are shown in B, and the *HPRT* promoter region was also analyzed. Results are the average of at least three independent experiments. *$p < 0.05$ and **$p < 0.005$.

TCS-SP5 confocal scanning microscope (Leica Microsystems, Mannheim, Germany) that was equipped with an HCX PLAPO 63× 1.4 oil immersion objective lens. Images of 20–30 serial optical sections, spaced by 0.25 μm, were acquired per cell nucleus. Approximately 250 nuclei were analyzed per cell type by using an "in-house" software (TIMT) that calculates the minimal distance though the three dimensions between heterochromatin and the FISH signal. To this end, the distribution of the heterochromatin and euchromatin domains (images recorded at 480 nm) as well as the position of the two FISH signals (images recorded at 570 nm) within the nucleus were first delimited and marked on the projection of all recorded sections by using Photoshop software (Adobe Systems, Mountain View, CA). The distance between the FISH signal and the nearest heterochromatin domain was then searched and measured through the whole image stacks and normalized to the surface area of the nucleus (Hoechst staining). The *MEST* and *HPRT* probes were bacterial artificial chromosome (BAC) RP24-211G11 and BAC RP24-335G16, respectively.

Bisulfite Conversion

Five micrograms of genomic DNA was digested with EcoRI for 1 h at 37°C, purified, and denatured with 0.3 M NaOH for 10 min at 42°C. DNA was converted by adding a solution containing 0.55 mg of hydroquinine (Sigma Chemie, Deisenhofen, Germany) and 0.202 g of sodium hydrogen sulfite (Aldrich, Germany) at pH 5.05 for 15 h at 54°C. Converted DNA was purified with nucleospin columns (Macherey-Nagel, Düren, Germany) and denatured 10 min at RT with 0.3 M NaOH. DNA fragments were ethanol precipitated in presence of glycoblue (Invitrogen) and cloned in blunt-ended pBluescript.

RESULTS

Identification of MEST as a TIF1β Primary Target Gene

To identify TIF1β endogenous target genes, we compared the transcriptome of WT F9 cells with that of the previously described *TIF1*$\beta^{HP1box/-}$ F9 cells expressing a mutated TIF1β protein (TIF1β^{HP1box}) unable to interact with HP1 (Cammas *et al*., 2004). The *MEST* gene displayed one of the highest -fold induction in mutant cells compared with WT cells (data not shown). To validate this microarray analysis, we performed quantitative (q)RT-PCR analysis with *MEST*-specific primers on RNA prepared from *TIF1*$\beta^{+/-}$ and *TIF1*$\beta^{HP1box/-}$ cells (Figure 1A). *MEST* expression is undetectable in *TIF1*$\beta^{+/-}$ cells, whereas it is highly expressed in *TIF1*$\beta^{HP1box/-}$ cells, confirming the microarray analysis and demonstrating that *MEST* repression requires the interaction between TIF1β and HP1 within F9 EC cells (Figure 1A). *MEST* is an imprinted gene also known as paternally expressed gene 1 (*PEG1*) (Kaneko-Ishino *et al*., 1995). It was therefore important to investigate whether TIF1β could be a specific regulator of imprinted genes. To this end, we analyzed the expression of several imprinted genes (Murphy and Jirtle, 2003) by using our preliminary microarrays analysis. On the 50 imprinted genes spotted on the microarray, 19 (38%) were found to be up-regulated and none down-regulated in *TIF1*$\beta^{HP1box/-}$ compared with *TIF1*$\beta^{+/-}$ cells (with a criteria of a >2-fold change with a p value; $p < 0.05$), whereas on the whole 25,785 genes spotted on the microarray, 3580 (14%) and 31 (0.1%) were up- and down-regulated, respectively, in *TIF1*$\beta^{HP1box/-}$ compared with *TIF1*$\beta^{+/-}$ cells by using the criteria described above (data not shown). The expression of four imprinted genes that was predicted by our preliminary microarray analysis to be either not modified (*PEG3* and *PEG10*) or induced (*IGF2R* and *MEG3*)

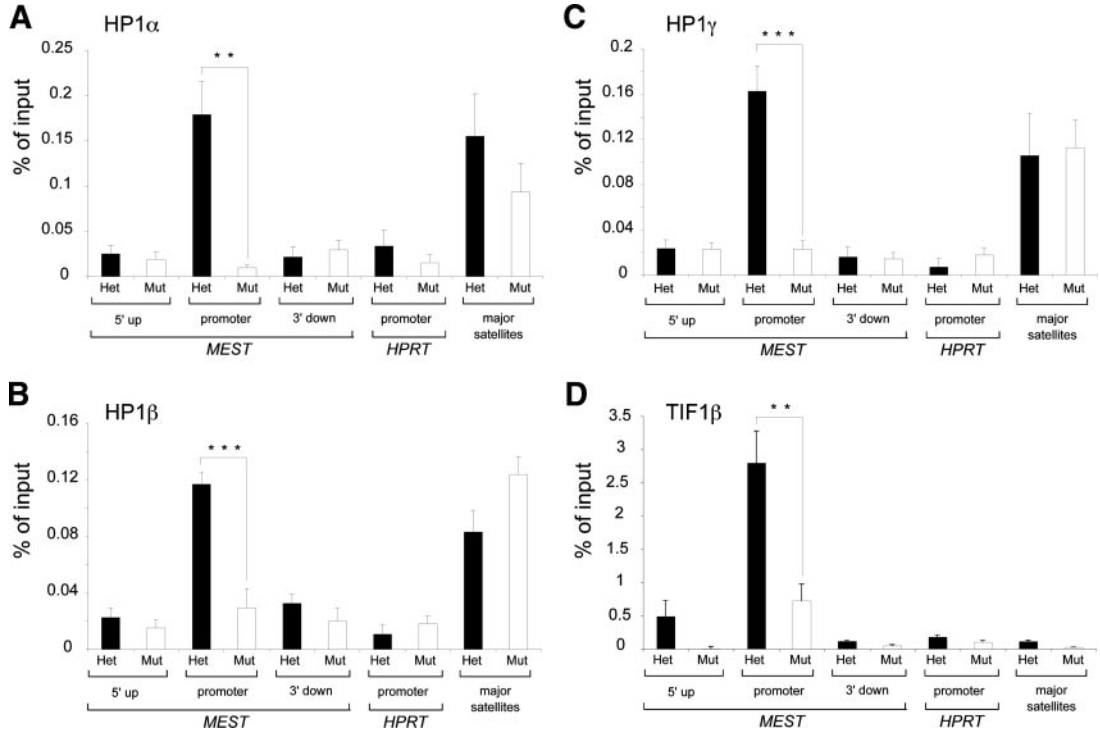

Figure 2. The interaction between TIF1β and HP1 is essential for TIF1β and HP1 recruitment to *MEST* promoter. ChIP assays were performed on *TIF1β*$^{+/-}$ cells (black bars; Het) and *TIF1β*$^{HP1box/-}$ cells (white bars; Mut) with antibodies directed against HP1α (A), HP1β (B), HP1γ (C), and TIF1β (D). PCR was performed with primers specific to the three *MEST* gene positions described in Figure 1B, the *HPRT* promoter, and the major satellites. *$p < 0.05$, **$p < 0.005$, and ***$p < 0.0005$.

in *TIF1β*$^{HP1box/-}$ compared with *TIF1β*$^{+/-}$ cells was validated by qRT-PCR (Figure 1A). These results indicate that TIF1β regulates either directly or indirectly the expression of a large number of genes, including a significant proportion of imprinted genes. We also measured the expression of *COPG2* whose 3′-untranslated region (UTR) overlaps *MEST* 3′-UTR on the mouse chromosome 6 (Lee *et al.*, 2000). This gene is expressed at a slightly, although not statistically significant, higher level in *TIF1β*$^{HP1box/-}$ compared with *TIF1β*$^{+/-}$ cells, implicating that TIF1β-HP1 is specifically involved in the regulation of *MEST* gene expression within this chromosomal locus (Figure 1A). To assess the regulation of *MEST* gene expression during differentiation, *TIF1β*$^{+/-}$ and *TIF1β*$^{HP1box/-}$ cells were treated for 4 d with 1 μM RA to induce PrE. qRT-PCR analysis shows that *MEST* expression is equivalently induced in both genetic backgrounds and remains 10^4 lower in *TIF1β*$^{+/-}$ cells than in *TIF1β*$^{HP1box/-}$ cells (Figure 1, C and D). These results indicate that *MEST* expression is inducible during PrE differentiation through a TIF1β–HP1 interaction-independent mechanism. Therefore, *MEST* gene expression regulation was only analyzed in noninduced conditions.

To establish whether *MEST* is a direct TIF1β target gene, we performed ChIP in WT F9 cells with two independent TIF1β antibodies, the monoclonal 1TB3 (Nielsen *et al.*, 1999; Figure 1E, m) and the polyclonal PF64 (Cammas *et al.*, 2002; Figure 1E, p) followed by real-time PCR. Results are represented as (signal with specific antibodies − signal with no antibody) normalized with the initial materials (input). TIF1β is significantly enriched on the *MEST* promoter region compared with regions 3.9 kb upstream and 6.3 kb downstream of this *MEST* promoter region as well as to the promoter region of the constitutively active *HPRT* gene (10.5; 17.4- and 12.5-fold, respectively, with the mAb; Figure 1E). These data strongly suggest that, in EC F9 cells, *MEST* is a primary target of TIF1β that maintains repression of this gene via a mechanism requiring its interaction with HP1.

The Interaction between TIF1β and HP1 Is Essential for Stable Recruitment of Both TIF1β and HP1 to MEST Promoter

To investigate the recruitment of HP1 to an endogenous TIF1β target gene, we performed ChIP with antibodies specific of the three HP1 isotypes, HP1α, HP1β, and HP1γ, in *TIF1β*$^{+/-}$ F9 cells. All three HP1 isotypes are significantly enriched on the *MEST* promoter region, whereas they are not significantly enriched in the 5′ upstream or 3′ downstream positions (Figure 2, A–C, Het). None of the HP1 isotypes are significantly recruited to the promoter of the *HPRT* gene, whereas all of them are, as expected, recruited to the constitutive heterochromatic major satellites, confirming that the signals detected on *MEST* promoter correspond to specific recruitment of the three HP1 isotypes (Figure 2, A–C). Furthermore, to determine whether the interaction between TIF1β and HP1 is required for HP1 recruitment to the *MEST* promoter, the same ChIPs were performed in *TIF1β*$^{HP1box/-}$ cells. As illustrated on Figure 2, A–C (Mut), no HP1 is significantly detected at any position of the *MEST* gene after ChIP with HP1α, HP1β, or HP1γ antibodies within *TIF1β*$^{HP1box/-}$ cells. In contrast, all three HP1 isotypes are still clearly detectable on the major satellites at a level equivalent to that observed in *TIF1β*$^{+/-}$ cells (Figure 2, A–C). This demonstrates that the interaction between TIF1β and HP1 is essential for specific HP1 recruitment to the *MEST* promoter, whereas it is not involved in the recruit-

ment of these proteins to the constitutive heterochromatic major satellites.

To determine whether the interaction between TIF1β and HP1 is also involved in the recruitment of TIF1β to the *MEST* promoter, ChIPs with the two TIF1β Abs, was performed in *TIF1*$\beta^{+/-}$ and *TIF1*$\beta^{HP1box/-}$ cells. Surprisingly, TIF1β^{HP1box} recruitment to *MEST* promoter is drastically decreased compared with the recruitment of TIF1β in *TIF1*$\beta^{+/-}$ cells, although it remains significantly above the signal detected on the *HPRT* promoter and on the major satellites sequences (Figure 2D; data not shown). This strongly suggests that the interaction between TIF1β and HP1 is not only essential for the recruitment of HP1 to the *MEST* promoter, but also for efficient TIF1β recruitment and/or stabilization to this region. Altogether, these data indicate that TIF1β and HP1 are recruited to *MEST* promoter through a mechanism that requires their mutual interaction to maintain gene repression within F9 EC cells.

TIF1β, through Its Interaction with HP1, Maintains a Heterochromatin-like Structure on the MEST Promoter

MEST is an imprinted gene that possesses a CpG island in its promoter region (Lefebvre *et al*., 1997; Figure 1B). It was therefore important to assess the DNA methylation status of this *MEST* CpG island in *TIF1*$\beta^{+/-}$ and *TIF1*$\beta^{HP1box/-}$ cells. To this end, we performed bisulfite sequencing and analyzed the methylation status of the *MEST* gene from position −455 base pairs to +269 base pairs comprising 56 CpG dinucleotides. This region of the *MEST* gene is fully methylated on both alleles in *TIF1*$\beta^{+/-}$ cells (Figure 3A). A notable exception to this full methylation pattern is the first position upstream to the transcription start site (at −33 base pairs) that is methylated in only 60% of *MEST* alleles (Figure 3A). In contrast to *TIF1*$\beta^{+/-}$ cells, only ~50% of *MEST* alleles are methylated within the CpG island in *TIF1*$\beta^{HP1box/-}$ cells (Figure 3A). This loss of *MEST* gene methylation is not a consequence of a general demethylation process within *TIF1*$\beta^{HP1box/-}$ cells, because digest of *TIF1*$\beta^{+/-}$ and *TIF1*$\beta^{HP1box/-}$ genomic DNA by the methylation-sensitive enzyme *Hpa*2 shows the same pattern on agarose gel (data not shown).

To establish the profile of histone modifications induced by TIF1β–HP1 recruitment to *MEST* promoter, we performed ChIP with antibodies specific of different histone modifications in *TIF1*$\beta^{+/-}$ cells. This analysis reveals that *MEST* promoter is highly enriched in 3meH3K9 and 3meH4K20, two modifications well known to be associated with heterochromatin structures and gene silencing (Figure 3B). Interestingly, 3meH3K9 and to a lesser extent 3meH4K20 specifically spreads up to 4 kb upstream from the promoter region (Figure 3B). These two marks are absent of the promoter region of the actively transcribed *HPRT* gene and highly enriched in the heterochromatic major satellite sequences demonstrating the specificity of the ChIP (Figure 3B). Furthermore, acetylation of H3K9 (AcH3K9), a mark associated with gene expression, is not significantly enriched on *MEST* promoter region of *TIF1*$\beta^{+/-}$ cells, whereas it is highly enriched on the promoter region of the constitutively transcribed *HPRT* (Figure 3B). As expected, this mark is also absent at the silent heterochromatic major satellites. Last, we analyzed the enrichment in 3meH3K27. 3meH3K27 is not significantly enriched within neither the *MEST* promoter, or the *HPRT* promoter or the heterochromatic major satellite sequences (Figure 3B). It is noteworthy that AcH3K9 and 3meH3K27 are slightly, although significantly, enriched 4 and 10 kb upstream the *MEST* promoter region within *TIF1*$\beta^{+/-}$ cells (Figure 3B). To demonstrate the specific role of TIF1β interaction with HP1 in the maintenance of this chromatin structure, the same ChIP experiments were performed in *TIF1*$\beta^{HP1box/-}$ cells. As expected, considering the loss of *MEST* repression in this cell line, 3meH3K9 and 3meH4K20 are lost from the *MEST* gene in *TIF1*$\beta^{HP1box/-}$ cells, with a concomitant enrichment of AcH3K9. More surprisingly, 3meH3K27 becomes highly enriched in the *MEST* promoter region and at 4 kb upstream this region (11.9- and 6-fold, respectively, compared with the signal in *TIF1*$\beta^{+/-}$ cells). This phenomenon is specific of the *MEST* promoter and its 4 kb upstream region since none of the histone modifications presented above are significantly altered at 10 kb upstream the *MEST* promoter region nor within the *HPRT* promoter nor the major satellite sequences in *TIF1*$\beta^{HP1box/-}$ compared with *TIF1*$\beta^{+/-}$ cells. To find out whether the 3meH3K27 mark that occurs specifically in *TIF1*$\beta^{HP1box/-}$ cells displays any preferential association with the methylated or unmethylated *MEST* allele, we performed bisulfite sequencing after a 3meH3K27 ChIP in *TIF1*$\beta^{HP1box/-}$ cells. As illustrated on Figure 3C, 3meH3K27 is exclusively associated with the unmethylated *MEST* allele.

MEST Preferentially Associates with Pericentromeric Heterochromatin in a TIF1β–HP1 Interaction-dependent Manner

It has been suggested that nuclear organization and in particular the localization of specific genomic loci close to heterochromatin has important implications for gene silencing (Brown *et al*., 1999). We therefore assessed the localization of the *MEST* gene within *TIF1*$\beta^{+/-}$ and *TIF1*$\beta^{HP1box/-}$ cells by FISH and confocal microscopy. The distance between the spots corresponding to the hybridization of the *MEST* gene to the nearest heterochromatin domain defined as bright spots of Hoechst staining was determined throughout the three dimensions of the nucleus using an in-house (TIMT) software. The distance was normalized by the surface of the nucleus. In both cell lines, three types of nuclei were observed: 1) both *MEST* alleles associated with heterochromatin (2HC), 2) both *MEST* alleles excluded from heterochromatin (2EU), and 3) one *MEST* allele within heterochromatin and one excluded from this compartment (1HC + 1EU) (Figure 3D). Interestingly, the proportion of the (1EU + 1HC) and (2EU) populations are significantly different within *TIF1*$\beta^{+/-}$ and *TIF1*$\beta^{HP1box/-}$ cells lines according to the statistical chi-square test ($\chi^2 < 0.01$), whereas the (2HC) populations are equivalently represented in both cell lines (7.1 and 10.2% in *TIF1*$\beta^{+/-}$ and *TIF1*$\beta^{HP1box/-}$ cells, respectively). The (1EU + 1HC) population represents 46.5% of *TIF1*$\beta^{+/-}$ cells, whereas it is found in only 24% of *TIF1*$\beta^{HP1box/-}$ cells (Figure 3D). Furthermore 43.3% of *TIF1*$\beta^{+/-}$ cells are (2EU) compared with 68.9% for *TIF1*$\beta^{HP1box/-}$ cells (Figure 3D). These changes are unlikely to result from a global difference of heterochromatin distribution between the two cell lines because no obvious difference is observed by Hoechst staining. Finally the average distance between the "EU" spots and the nearest heterochromatin domain is equivalent in both genetic backgrounds (0.952 and 0.895 μm in *TIF1*$\beta^{+/-}$ and *TIF1*$\beta^{HP1box/-}$ cells, respectively) (Figure 3D). Furthermore, we analyzed the subnuclear localization of the chromosome X-associated gene, *HPRT*, and we found that this gene is euchromatic in 84.4 and 85.9% of *TIF1*$\beta^{+/-}$ and *TIF1*$\beta^{HP1box/-}$ nuclei, respectively (data not shown). These data strongly suggest that the association of TIF1β with HP1 facilitates the anchorage of the *MEST* locus within pericentromeric heterochromatin.

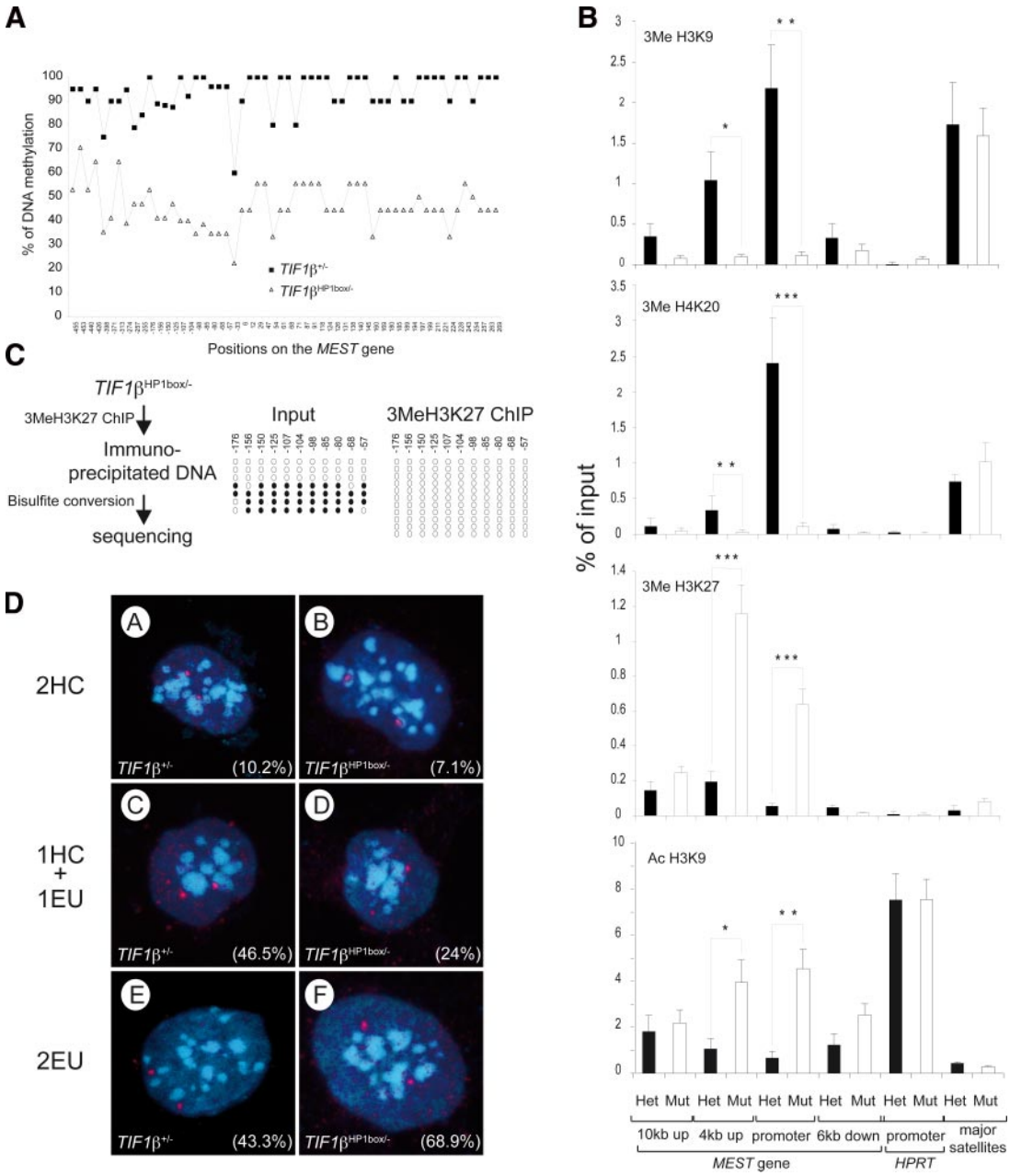

Figure 3. TIF1β, through its interaction with HP1, maintains a heterochromatin-like structure on the *MEST* promoter. (A) DNA methylation of the *MEST* CpG island from position −455 base pairs to position 269 base pairs was analyzed in $TIF1\beta^{+/-}$ (black square) and $TIF1\beta^{HP1box/-}$ F9 cell lines (open triangles) by bisulfite sequencing. (B) The histone modification status of *MEST* promoter and of its surrounding regions, of the *HPRT* promoter and of the major satellite sequences were analyzed by ChIP in nontreated $TIF1\beta^{+/-}$ (black bars; Het) and $TIF1\beta^{HP1box/-}$ F9 cell lines (white bars; Mut). As annotated trimethylation of H3K9 (3meH3K9), H4K20 (3meH4K20), H3K27 (3meH3K27) and acetylation of H3K9 (AcH3K9) were assessed. (C) The DNA methylation status of the *MEST* promoter region associated with 3meH3K27 was assessed by bisulfite sequencing after ChIP with an anti-3meH3K27 pAb in $TIF1\beta^{HP1box/-}$ cells. The open circles represent the unmethylated CpG and the black circles the methylated CpG. (D) DNA FISH analysis was performed using a *MEST* gene specific probe in $TIF1\beta^{+/-}$ and $TIF1\beta^{HP1box/-}$ F9 cell lines (red dots). Pericentromeric heterochromatin was labeled by Hoechst staining and occurs as bright blue spots. Representative cells with two spots within heterochromatin (A and B), one spot within euchromatin and one spot within heterochromatin (C and D) or two spots within euchromatin (E and F) are shown. The percentages represent the analysis of >250 cells for each genotype. *$p < 0.05$, **$p < 0.005$, and ***$p < 0.0005$.

TIF1β Is Permanently Required on MEST Promoter to Maintain Transcriptional Repression

To address the kinetic of loss of TIF1β-mediated *MEST* repression upon disruption of TIF1β–HP1 interaction, we established a cell line allowing hydroxytamoxifen (OHT)-inducible disruption of the interaction between these two proteins. This cell line ($TIF1\beta^{L2/HP1box}$/*Cre-ER*^{T2}) carries 1) one floxed *TIF1β* allele ($TIF1\beta^{L2}$), 2) the other *TIF1β* allele with the HP1box motif mutated by homologous recombination ($TIF1\beta^{HP1box}$), and 3) an expression vector driving stable expression of the OHT-inducible CreER^{T2} recombinase (Indra *et al.*, 1999). These cells were treated for different

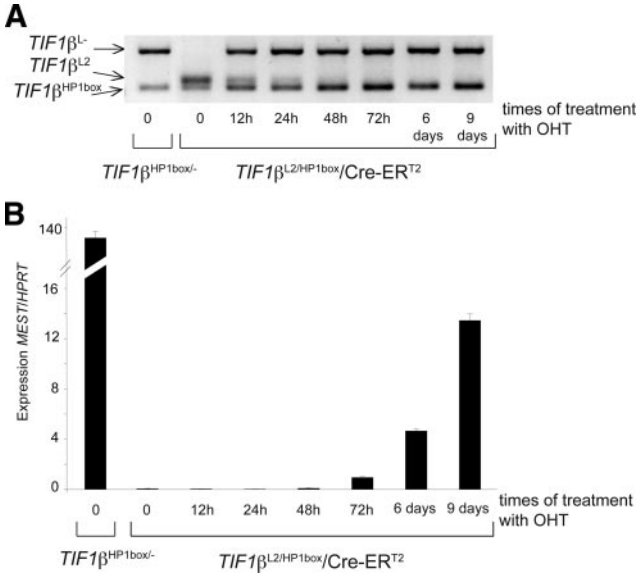

Figure 4. TIF1β-HP1 interaction is permanently required to maintain *MEST* repression. *TIF1β*$^{L2/HP1box}$*/CreER*^{T2} cells were treated for the indicated times with 10^{-7} M OHT and collected for RNA and DNA preparations. (A) Cells were genotyped at each time point by PCR as described previously (Cammas *et al*., 2004). (B) *MEST* expression was measured by qRT-PCR at each time and normalized by *HPRT* expression.

times with OHT and collected for genotyping and analysis of *MEST* expression. Excision of the floxed *TIF1β*^{L2} allele was detectable as early as 12 h of OHT treatment and 48 h of OHT treatment were sufficient to detect *MEST* expression, which was further increased by 122-fold until 9 d of OHT treatment (Figure 4, A and B). It is noteworthy, that, although *MEST* expression increases with time after OHT treatment, it only reaches 10% of the level obtained in *TIF1β*$^{HP1box/-}$ cells (data not shown). These results indicate that *MEST* repression is rapidly lost upon disruption of the interaction between TIF1β and HP1 and strongly suggest that the interaction between these two proteins is permanently required to maintain *MEST* repression.

TIF1β Is Sufficient to Establish the Heterochromatin-like Structure on MEST Gene

As described above, TIF1β, through its interaction with HP1, is essential to maintain *MEST* repression. A key question that remained to be answered was whether TIF1β is also involved for the establishment of *MEST* repression. To address this question, we used the previously established cell line *TIF1β*$^{HP1box/-}$*/rTA-f.TIF1β* allowing inducible expression of FLAG-TIF1β (f.TIF1β) by doxycycline (Dox) treatment within *TIF1β*$^{HP1box/-}$ cells (Cammas *et al*., 2004). f.TIF1β expression was verified by Western using the anti-FLAG mAb in *TIF1β*$^{HP1box/-}$*/rTA-f.TIF1β* cells. As expected, f.TIF1β is expressed only in presence of Dox; however, this does not lead to any significant increase in the total level of TIF1β in these cells, strongly suggesting that f.TIF1β level is very low compared with endogenous TIF1β (Figure 5A). f.TIF1β expression was also verified by immunofluorescence and found to be homogenous in each Dox-treated *TIF1β*$^{HP1box/-}$*/rTA-f.TIF1β* cell (data not shown). f.TIF1β recruitment to *MEST* promoter was then assessed by ChIP with the anti-FLAG antibody. As illustrated on Figure 5B, f.TIF1β is efficiently recruited to *MEST* promoter only in presence of Dox.

MEST expression was quantified in presence or absence of Dox treatment. Dox induces a twofold decrease of *MEST* expression compared with nontreated cells (Figure 5C), demonstrating that f.TIF1β is able to partially restore *MEST* repression. This twofold decrease in *MEST* expression was maintained even after 15 passages, strongly suggesting that these cells are refractory to further repression (data not shown), most likely due in part to the low level of f.TIF1β expression. It was then essential to determine whether f.TIF1β could reestablish the heterochromatin-like structure observed in *TIF1β*$^{+/-}$ cells. To this end, we analyzed specific histone modifications in *TIF1β*$^{HP1box/-}$*/rTA-f.TIF1β* cells in presence or absence of Dox treatment. ChIP experiments show that 3meH4K20 and 3meH3K9 are increased by 3.6- and 3.1-fold, respectively, in the promoter region of Dox-treated cells compared with nontreated cells, whereas 3meH3K27 and AcH3K9 are both decreased by 1.7-fold in these same conditions (Figure 5D). Although the amplitude of these changes is relatively limited, they demonstrate that f.TIF1β is able to reestablish to some extent the histone modification profile observed in *TIF1β*$^{+/-}$ cells. As mentioned above, the level of f.TIF1β is extremely low compared with that of the endogenous protein and might be a limiting factor for detection of DNA methylation by bisulfite sequencing. We therefore analyzed DNA methylation of the −176- to −57-bp region upstream the *MEST* transcription start site after immunoprecipitation of Dox-treated *TIF1β*$^{HP1box/-}$*/rTA-f.TIF1β* chromatin with the anti-FLAG mAb. As control, total DNA before ChIP (input) was also analyzed. As shown on Figure 5E, ~100% of the *MEST* alleles associated with f.TIF1β are methylated, whereas only ~50% are methylated in the input. This demonstrates that f.TIF1β is able to establish DNA methylation at the *MEST* promoter; however, most likely because of the low level of f.TIF1β expression, this rescue is undetectable on total *TIF1β*$^{HP1box/-}$*/rTA-f.TIF1β* cell DNA.

MEST Proximal Promoter Region Is Highly Methylated in Liver

It has been suggested that several imprinted loci become aberrantly methylated on both alleles in F9 cells (Yeivin *et al*., 1996). To decipher whether the full methylation of *MEST* observed in our F9 model corresponds to any physiological condition, we tested *MEST* expression in different adult mouse tissues. As shown previously, *MEST* expression is very low in all tissues and in particular in liver in which *MEST* expression is 19-fold lower than in *TIF1β*$^{HP1box/-}$ F9 cells (Figure 6A; data not shown; Lui *et al*., 2008). We analyzed the methylation status of the *MEST* promoter region in adult liver. As illustrated on Figure 6B, bisulfite sequencing analysis shows that the *MEST* promoter region between −107 and −57 bp is methylated on 90% of the alleles. These results strongly suggest that, as in F9 EC cells, *MEST* proximal promoter region is methylated on both alleles.

DISCUSSION

In this study, we identified the *MEST* gene as an endogenous TIF1β primary target gene in embryonal carcinoma F9 cells. We demonstrate that the interaction between TIF1β and HP1 proteins is critical for *MEST* repression, being essential for mutual recruitment and/or stabilization of both proteins on the promoter region. We further show that TIF1β–HP1 interaction is critical for the maintenance and the establishment of a local heterochromatin-like structure characterized by H3K9 trimethylation and hypoacetylation, H4K20 trimethylation, DNA hypermethylation, and enrich-

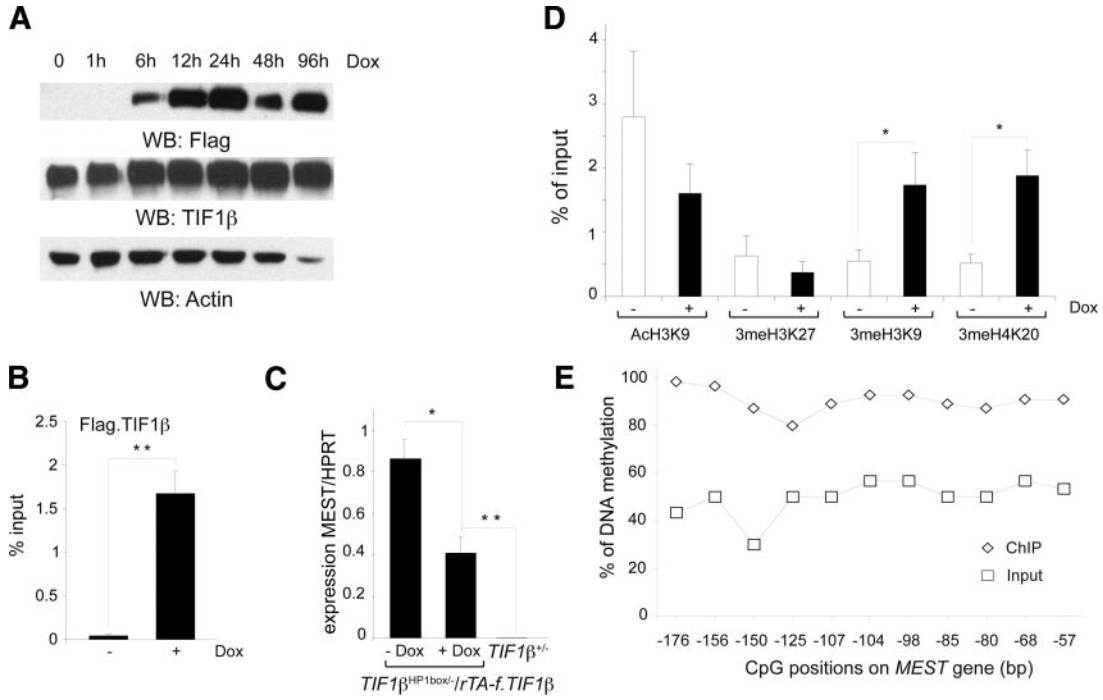

Figure 5. Flag-TIF1β expression partially rescues *MEST* repression. (A) Western blot analysis of f.TIF1β expression was performed on *TIF1β*$^{HP1box/-}$*/rTA-f.TIF1β* cells treated for the indicated times with Dox by using an anti-FLAG antibody. Total TIF1β expression was also assessed with an anti-TIF1β antibody. Protein loading was controlled with an anti-actin antibody. (B) ChIP using an anti-FLAG antibody was performed on *TIF1β*$^{HP1box/-}$*/rTA-f.TIF1β* cells in absence or presence of Dox. (C) *MEST* expression was assessed by qRT-PCR in *TIF1β*$^{HP1box/-}$*/rTA-f.TIF1β* cells treated or not with Dox and in *TIF1β*$^{+/-}$ cells. *MEST* expression was normalized with *HPRT*. (D) ChIP with antibodies of the specified histone modifications were performed on *TIF1β*$^{HP1box/-}$*/rTA-f.TIF1β* cells in presence or absence of Dox. (E) DNA methylation was assessed by bisulfite sequencing in *TIF1β*$^{HP1box/-}$*/rTA-f.TIF1β* after ChIP with an anti-FLAG mAb. The open lozenges represent the analysis of the ChIP genomic DNA and the open squares the input. *$p < 0.05$ and **$p < 0.005$.

ment in HP1. This structure correlates with a preferential association of the *MEST* gene to foci of pericentromeric heterochromatin and *MEST* repression.

Interestingly, *MEST* is an imprinted gene, and three of our results strongly suggest that TIF1β regulates only one of the two *MEST* alleles: 1) although both alleles are fully methylated in *TIF1β*$^{+/-}$ EC F9 cells, only 50% of the *MEST* fragments sequenced are methylated in *TIF1β*$^{HP1box/-}$, strongly suggesting that only one allele is demethylated upon disruption of the interaction between TIF1β and HP1; 2) only one of the two alleles seems to be significantly associated with pericentromeric heterochromatic foci, a localization that requires the interaction between TIF1β and HP1; and 3) upon disruption of the interaction between TIF1β and HP1, there is a switch from high levels of 3meH3K9 and 3meH4K20 and low level of 3meH3K27 to low levels of 3meH3K9 and 3meH4K20 and high level of 3meH3K27 that is exclusively associated with the demethylated *MEST* allele. These results indicate that the two *MEST* alleles are clearly silenced by two different mechanisms that both rely on DNA methylation, but of which, only one involves the formation of a heterochromatin-like structure and is dependent upon the interaction between TIF1β and HP1. Because 50% of *MEST* methylation is refractory to TIF1β loss of function, it is very likely that TIF1β does not regulate the allele of maternal origin that is imprinted but rather the paternal nonimprinted allele. This strongly suggests that the molecular mechanisms of gene repression described in this study apply to both imprinted and nonimprinted genes, a conclusion in line with the large number of imprinted and nonimprinted genes up-regulated upon loss of interaction between TIF1β and HP1. Very interestingly, we show in liver that the *MEST* proximal promoter region between −107 and −57 base pairs is methylated on 90% of the alleles, which correlates with a very low level of *MEST* expression. This result is in striking contrast with the observation made on the *MEST* distal promoter region (−1001 to −792 bp) that is methylated only on 50% of *MEST* alleles (Lui *et al.*, 2008). The different methylation status between these two *MEST* promoter regions strongly suggests that there is a boundary element between –792 and –107 base pairs that inhibits DNA methylation spreading on the nonimprinted allele but not on the imprinted alleles that is methylated, even on the *MEST* distal promoter. Together, these results highlight the existence of different mechanisms of DNA methylation establishment and/or maintenance. The marks that allow the preferential association of TIF1β with the nonimprinted allele and the establishment and/or maintenance of DNA methylation on specific gene area remain to be elucidated, but most likely they involve a complex combinatorial presence of histone modifications on each *MEST* allele. This is the first demonstration that the nonimprinted allele of an imprinted gene is regulated by DNA methylation in vivo.

Concerning the molecular mechanism underlying TIF1β functions as a corepressor, it is interesting to note that, although 3meH3K9 and to a lesser extent 3meH4K20 extend around 4kb upstream the *MEST* transcription start site, HP1 binding is limited to the proximal *MEST* promoter region, indicating that, in contrast to constitutive heterochromatin, HP1 is not spreading to surrounding regions and that 3meH3K9 and 3meH4K20 on their own are not sufficient for HP1 recruitment. This conclusion is in agreement with the

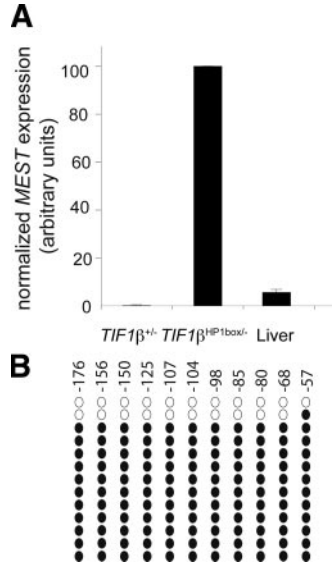

Figure 6. MEST proximal promoter region is hypermethylated in liver. (A) qRT-PCR analysis of *MEST* expression in $TIF1\beta^{+/-}$ and $TIF1\beta^{HP1box/-}$ F9 cells and adult liver. Results are normalized with *HPRT* expression and shown as arbitrary units. (B) *MEST* proximal promoter region is highly methylated in adult liver. Methylation of the *MEST* promoter region between −107 and −57 base pairs was analyzed by bisulfite sequencing on genomic DNA prepared from three independent adult animal livers. The illustration of a representative experiment on an adult liver is shown. The open circles represent the unmethylated CpG, and the closed circles the methylated CpG.

finding that in heterochromatin, HP1 association to chromatin requires both H3K9 trimethylation and direct association with Suv39H1 (Stewart *et al*., 2005). It is very likely that, here, HP1 chromatin association necessitates both H3K9 trimethylation and direct binding to TIF1β. Furthermore, we find that *MEST* repression is rapidly lost upon disruption of the interaction between TIF1β and HP1 strongly suggesting that this repression requires permanent loading of TIF1β on *MEST* promoter region. This is in contrast with studies using integrated artificial TIF1β target genes, in which the authors concluded that a single pulse of TIF1β expression allowed transgene silencing for several passages (Sripathy *et al*., 2006). These data clearly demonstrates that HP1 loading on *MEST* promoter for repression can rapidly be displaced for gene activation. The loss of HP1 on *MEST* promoter is accompanied by loss of 3meH3K9, 3meH4K20, DNA methylation and a gain of 3meH3K27, demonstrating that all these chromatin modifications are very dynamic and interdependent as previously suggested in other systems (Freitag *et al*., 2004; Smallwood *et al*., 2007; Wu *et al*., 2008). This conclusion is also in line with studies indicating that HP1 distribution within the nucleus is highly dynamic (Cheutin *et al*., 2003) and that DNA methylation is not always as stably established as assumed previously (Kangaspeska *et al*., 2008; Métivier *et al*., 2008). It is also intriguing that in most studies 3meH3K27 is associated with gene silencing, whereas in the present study, 3meH3K27 is associated with gene activation in $TIF1\beta^{HP1box/-}$ cells. This association of 3meH3K27 with gene activation has, however, been observed in some cases and often correlates with loss of DNA methylation, suggesting that 3meH3K27 could be a "default mark" when DNA methylation is lost on genes normally regulated by the formation of a heterochromatin-like structure (Peters *et al*., 2003; Mathieu *et al*., 2005; McGarvey *et al*., 2006; Papp and Müller, 2006).

In conclusion, we have demonstrated that the expression of the imprinted *MEST* gene expression is tightly regulated by a complex interplay of epigenetic modifications and in particular by two distinct DNA methylation-dependent mechanisms of which, only one is dependent upon TIF1β.

ACKNOWLEDGMENTS

We thank Prof. A.J.L. Clark and Dr. I. Bogdarina, Saint Bartholomew's Hospital, London, United Kingdom, for helpful technical advice for bisulfite sequencing; S. Dumanoir for helpful technical advice for FISH analysis; and B. Jost, D. Dembele, and C. Bole-Feysot for help in the microarray analysis. We thank M. Cerviño for technical assistance; M. Beglin, J.-L., M. Koch, Y. Lutz, P. Kessler, and D. Hentsch for confocal laser scanning microscopy; S. Vicaire and D. Stephan for DNA sequencing; M. Oulad-Abdelghani for antibodies supply; and B. Heller for medium supply. This work was supported by the Centre National de la Recherche Scientifique, the Institut National de la Santé et de la Recherche Médicale, the Agence Nationale de la Recherche (ANR06-BLAN-0377), the Association pour la Recherche sur le Cancer, and the Collège de France. R. R. was supported by a fellowship from the Ministèrede la Recherche et de la Technologie.

REFERENCES

Abrink, M., Ortiz, J. A., Mark, M., Sanchez, C., Looman, C., Hellman, L., Chambon, P., and Losson, R. (2001). Conserved interaction between distinct Kruppel-associated box domains and the transcriptional intermediary factor 1 β. Proc. Natl. Acad. Sci. USA *98*, 1422–1426.

Ayyanathan, K., Lechner, M. S., Bell, P., Maul, G. G., Schultz, D. C., Yamada, Y., Tanaka, K., Torigoe, K., and Rauscher, F. J., 3rd (2003). Regulated recruitment of HP1 to a euchromatic gene induces mitotically heritable, epigenetic gene silencing: a mammalian cell culture model of gene variegation. Genes Dev. *17*, 1855–1869.

Boylan, J. F., and Gudas, L. J. (1991). Overexpression of the cellular retinoic acid binding protein-I (CRABP-I) results in a reduction in differentiation-specific gene expression in F9 teratocarcinoma cells. J. Cell Biol. *112*, 965–979.

Bracken, A. P., Dietrich, N., Pasini, D., Hansen, K. H., and Helin, K. (2006). Genome-wide mapping of Polycomb target genes unravels their roles in cell fate transitions. Genes Dev. *20*, 1123–1136.

Brown, K. E., Baxter, J., Graf, D., Merkenschlager, M., and Fisher, A. G. (1999). Dynamic repositioning of genes in the nucleus of lymphocytes preparing for cell division. Mol. Cell *3*, 207–217.

Cammas, F., Mark, M., Dollé, P., Dierich, A., Chambon, P., and Losson, R. (2000). Mice lacking the transcriptional corepressor TIF1β are defective in early postimplantation development. Development *127*, 2955–2963.

Cammas, F., Oulad-Abdelghani, M., Vonesch, J.-L., Chambon, P., and Losson, R. (2002). Cell differentiation induces TIF1βassociation with centromeric heterochromatin through HP1 interaction. J. Cell Sci. *115*, 3439–3448.

Cammas, F., Herzog, M., Lerouge, T., Chambon, P., and Losson, R. (2004). Association of the transcriptional corepressor TIF1β with Heterochromatin Protein 1 (HP1): an essential role for progression through differentiation. Genes Dev. *18*, 2147–2160.

Cammas, F., Janoshazi, A., Lerouge, T., and Losson, R. (2007). HP1 Dynamic and selective interactions of the transcriptional corepressor TIF1 beta with the heterochromatin protein HP1 isotypes during cell differentiation. Differentiation *7*, 627–637.

Cheutin, T., McNairn, A. J., Jenuwein, T., Gilbert, D. M., Singh, P. B., and Misteli, T. (2003). Maintenance of stable heterochromatin domains by dynamic HP1 binding. Science *299*, 721–725.

Chiba, H., Clifford, J., Metzger, D., and Chambon, P. (1997). Specific and redundant functions of retinoid X receptor/retinoic acid receptor heterodimers in differentiation, proliferation, and apoptosis of F9 embryonal carcinoma cells. Cell Biol. *139*, 735–747.

Cryderman, D. E., Grade, S. K., Li, Y., Fanti, L., Pimpinelli, S., and Wallrath, L. L. (2005). Role of *Drosophila* HP1 in euchromatic gene expression. Dev. Dyn. *232*, 767–774.

Eissenberg, J. C., James, T. C., Foster-Hartnett, D. M., Hartnett, T., Ngan, V., and Elgin, S. C. (1990). Mutation in a heterochromatin-specific chromosomal protein is associated with suppression of position-effect variegation in *Drosophila melanogaster*. Proc. Natl. Acad. Sci. USA *87*, 9923–9927.

Freitag, M., Hickey, P. C., Khlafallah, T. K., Read, N. D., and Selker, E. U. (2004). HP1 is essential for DNA methylation in *Neurospora*. Mol. Cell *13*, 427–434.

Friedman, J. R., Fredericks, W. J., Jensen, D. E., Speicher, D. W., Huang, X. P., Neilson, E. G., and Rauscher, F. J., 3rd (1996). KAP-1, a novel corepressor for the highly conserved KRAB repression domain, Genes Dev. *10*, 2067–2078.

Grewal, S. I., and Jia, S. (2007). Heterochromatin revisited. Nat. Rev. Genet. *8*, 35–46.

Hirose, S. (2007). Crucial roles for chromatin dynamics in cellular memory. J. Biochem. *14*, 615–619.

Indra, A. K., Warot, X., Brocard, J., Bornert, J. M., Xiao, J. H., Chambon, P., and Metzger, D. (1999). Temporally-controlled site-specific mutagenesis in the basal layer of the epidermis: comparison of the recombinase activity of the tamoxifen-inducible Cre-ER(T) and Cre-ER(T2) recombinases. Nucleic Acids Res. *27*, 4324–4327.

Kaneko-Ishino, T., Kuroiwa, Y., Miyoshi, N., Kohda, T., Suzuki, R., Yokoyama, M., Viville, S., Barton, S. C., Ishino, F., and Surani, M. A. (1995). Peg1/MEST imprinted gene on chromosome 6 identified by cDNA subtraction hybridization. Nat. Genet. *11*, 52–59.

Kangaspeska, S., Stride, B., Métivier, R., Polycarpou-Schwarz, M., Ibberson, D., Carmouche, R. P., Benes, V., Gannon, F., and Reid, G. (2008). Transient cyclical methylation of promoter DNA. Nature *452*, 112–115.

Kim, S. S., Chen, Y. M., O'Leary, E., Witzgall, R., Vidal, M., and Bonventre, J. V. (1996). A novel member of the RING finger family, KRIP-1, associates with the KRAB-A transcriptional repressor domain of zinc finger proteins, Proc. Natl. Acad. Sci. USA *93*, 15299–15304.

Latham, T., Gilbert, N., and Ramsahoye, B. (2008). DNA methylation in mouse embryonic stem cells and development. Cell Tissue Res. *331*, 31–55.

Le Douarin, B., Nielsen, A. L., Garnier, J.-M., Ichinose, H., Jeanmougin, F., Losson, R., and Chambon, P. (1996). A possible involvement of TIF1α and TIF1β in the epigenetic control of transcription by nuclear receptors. EMBO J. *15*, 6701–6715.

Lee, Y. J., Park, C. W., Hahn, Y., Park, J., Lee, J., Yun, J. H., Hyun, B., and Chung, J. H. (2000). Mit1/Lb9 and Copg2, new members of mouse imprinted genes closely linked to Peg1/MEST(1). FEBS Lett. *472*, 230–234.

Lefebvre, L., Viville, S., Barton, S. C., Ishino, F., and Surani, M. A. (1997). Genomic structure and parent-of-origin-specific methylation of Peg1. Hum. Mol. Genet. *6*, 1907–1915.

Lomberk, G., Wallrath, L., and Urrutia, R. (2006). The heterochromatin protein 1 family. Genome Biol. *7*, 228

Lui, J. C., Finkielstain, G. P., Barnes, K. M., and Baron, J. (2008). An imprinted gene network that controls mammalian somatic growth is down-regulated during postnatal growth deceleration in multiple organs. Am. J. Physiol. Regul. Integr. Comp. Physiol. *295*, R189–R196.

Mathieu, O., Probst, A. V., and Paszkowski, J. (2005). Distinct regulation of histone H3 methylation at lysines 27 and 9 by CpG methylation in *Arabidopsis*. EMBO J. *24*, 2783–2791.

McGarvey, K. M., Fahrner, J. A., Greene, E., Martens, J., Jenuwein, T., and Baylin, S. B. (2006). Silenced tumor suppressor genes reactivated by DNA demethylation do not return to a fully euchromatic chromatin state. Cancer Res. *66*, 3541–3549.

Mellor, J. (2006). Dynamic nucleosomes and gene transcription. Trends Genet. *22*, 320–329.

Métivier, R. *et al*. (2008). Cyclical DNA methylation of a transcriptionally active promoter. Nature *452*, 45–50.

Moosmann, P., Georgiev, O., Le Douarin, B., Bourquin, J. P., and Schaffner, W. (1996). Transcriptional repression by RING finger protein TIF1β that interacts with the KRAB repressor domain of KOX1. Nucleic Acids Res. *24*, 4859–4867.

Murphy, S. K., and Jirtle, R. L. (2003). Imprinting evolution and the price of silence. Bioessays *25*, 577–588.

Nielsen, A. L., Ortiz, J. A., You, J., Oulad-Abdelghani, M., Khechumian, R., Gansmuller, A., Chambon, P., and Losson, R. (1999). Interaction with members of the heterochromatin protein 1 (HP1) family and histone deacetylation are differentially involved in transcriptional silencing by members of the TIF1 family. EMBO J. *18*, 6385–6399.

Papp, B., and Müller, J. (2006). Histone trimethylation and the maintenance of transcriptional ON and OFF states by trxG and PcG proteins. Genes Dev. *20*, 2041–2054.

Peters, A. H. *et al*. (2003). Partitioning and plasticity of repressive histone methylation states in mammalian chromatin. Mol. Cell *12*, 1577–1589.

Rajasekhar, V. K., and Begemann, M. (2007). Concise review: roles of polycomb group proteins in development and disease: a stem cell perspective. Stem Cells *25*, 2498–2510.

Reik, W. (2007). Stability and flexibility of epigenetic gene regulation in mammalian development. Nature *447*, 425–432.

Ryan, R. F., Schultz, D. C., Ayyanathan, K., Singh, P. B., Friedman, J. R., Fredericks, W. J., and Rauscher, F. J. 3rd. (1999). KAP-1 corepressor protein interacts and colocalizes with heterochromatic and euchromatic HP1 proteins: a potential role for Krüppel-associated box-zinc finger proteins in heterochromatin-mediated gene silencing. Mol. Cell. Biol. *19*, 4366–4378.

Schotta, G., Lachner, M., Sarma, K., Ebert, A., Sengupta, R., Reuter, G., Reinberg, D., and Jenuwein, T. (2004). A silencing pathway to induce H3–K9 and H4–K20 trimethylation at constitutive heterochromatin. Genes Dev. *18*, 1251–1262.

Schultz, D. C., Friedman, J. R., and Rauscher, F. J. 3rd. (2001). Targeting histone deacetylase complexes via KRAB-zinc finger proteins: the PHD and bromodomains of KAP-1 form a cooperative unit that recruits a novel isoform of the Mi-2α subunit of NuRD. Genes Dev. *15*, 428–443.

Schultz, D. C., Ayyanathan, K., Negorev, D., Maul, G. G., and Rauscher, F. J., 3rd (2002). SETDB 1, a novel KAP-1-associated histone H3, lysine 9-specific methyltransferase that contributes to HP1-mediated silencing of euchromatic genes by KRAB zinc-finger proteins. Genes Dev. *16*, 919–932.

Smallwood, A., Esteve, P. O., Pradhan, S., and Carey, M. (2007). Functional cooperation between HP1 and DNMT1 mediates gene silencing. Genes Dev. *21*, 1169–1178.

Song, F., Smith, J. F., Kimura, M. T., Morrow, A. D., Matsuyama, T., Nagase, H., and Held, W. A. (2005). Association of tissue-specific differentially methylated regions (TDMs) with differential gene expression. Proc. Natl. Acad. Sci. USA *102*, 3336–3341.

Sripathy, S. P., Stevens, J., and Schultz, D. C. (2006). The KAP1 corepressor functions to coordinate the assembly of de novo HP1-demarcated microenvironments of heterochromatin required for KRAB zinc finger protein-mediated transcriptional repression. Mol. Cell. Biol. *26*, 8623–8638.

Stewart, M. D., Li, J., and Wong, J. (2005). Relationship between histone H3 lysine 9 methylation, transcription repression, and heterochromatin protein 1 recruitment. Mol. Cell. Biol. *25*, 2525–2538.

Thiru, A., Nietlispach, D., Mott, H. R., Okuwaki, M., Lyon, D., Nielsen, P. R., Hirshberg, M., Verreault, A., Murzina, N. V., and Laue, E. D. (2004). Structural basis of HP1/PXVXL motif peptide interactions and HP1 localisation to heterochromatin. EMBO J. *23*, 489–499.

Underhill, C., Qutob, M. S., Yee, S.-P., and Torchia, J. (2000). A novel nuclear receptor corepressor complex, N-CoR, contains components of the mammalian SWI/SNF complex and the corepressor KAP-1. J. Biol. Chem. *275*, 40463–40470.

Vakoc, C. R., Mandat, S. A., Olenchock, B. A., and Blobel, G. A. (2005). Histone H3 lysine 9 methylation and HP1gamma are associated with transcription elongation through mammalian chromatin. Mol. Cell *19*, 381–391.

Wang, G., Ma, A., Chow, C. M., Horsley, D., Brown, N. R., Cowell, I. G., and Singh, P. B. (2000). Conservation of heterochromatin protein 1 function. Mol. Cell. Biol. *20*, 6970–6983.

Weber, M., Hellmann, I., Stadler, M. B., Ramos, L., Pääbo, S., Rebhan, M., and Schübeler, D. (2007). Distribution, silencing potential and evolutionary impact of promoter DNA methylation in the human genome. Nat. Genet. *39*, 457–466.

Wu, L. P. *et al*. (2008). HDAC inhibitor depsipeptide activates silenced genes through decreasing both CpG and H3K9 methylation on the promoter. Mol. Cell. Biol. *28*, 3219–3235.

Yeivin, A., Levine, A., and Razin, A. (1996). DNA methylation patterns in tumors derived from F9 cells resemble methylation at the blastula stage. FEBS Lett. *395*, 11–16.